PURITY DETERMINATION USING DSC

11.1 Introduction

Measurements of the depression of the melting point [1] of a sample are often used to determine its purity [2]. Melting endotherms, recorded using differential scanning calorimetry (DSC), are routinely used to recognize the occurrence of melting and to measure the melting temperature of the sample. With a bit more effort, as discussed below, it is possible to determine the purity of the sample by analyzing, in detail, the shape of the melting endotherm. There is no need to have a high-purity sample of the substance under investigation for comparison, although a sample of any very pure material, such as indium metal, is needed to determine the thermal performance of the particular instrument being used. Because such materials are used, in any case, to calibrate the instrument for temperature and enthalpy measurements, this last requirement is readily achievable. Calculations are based on the assumptions that solid solutions are not formed and that the melt is an ideal solution. Melting must not be accompanied by decomposition or sublimation. The assumptions made apply only to relatively pure (>98%) materials.

The practical aim of purity determinations is usually to decide whether or not the sample meets certain specifications, determined by the intended further uses of the sample. Special Technical Publication 838 of the ASTM [3] is an important source of information on purity determination. In it, a review by Brennan and co-workers [4] outlines the history of the DSC method and emphasizes A.P. Gray's pioneering work in this area.

The melting endotherm for a pure substance recorded on a DSC is illustrated in Figure 11.1. T_o is the melting point of the sample and the area ABC is proportional to the enthalpy of fusion, ΔH_{fus}, of the sample. The presence of an impurity in the sample (the solvent) generally lowers the melting point of the solvent and also broadens the melting range, giving a broader DSC endotherm as illustrated in Figure 11.2 (inset). From endotherms such as illustrated in Figures 11.1 and 11.2, melting points and enthalpies of fusion may readily be determined. In suitable cases, as mentioned above, an estimate of the purity of a compound can be obtained, from analysis of the detailed shape of its melting endotherm, e.g., Figure 11.2, without reference to compounds containing known amounts of impurities.

Figure 11.1
Idealized DSC record of the melting of pure indium. Slope AB ($=1/R_0$) is used to correct for the thermal lag. T_o is the melting point of the sample and the area ABC is proportional to the enthalpy of fusion, ΔH_{fus}, of the sample [2]. (With the permission of the Journal of Chemical Education.)

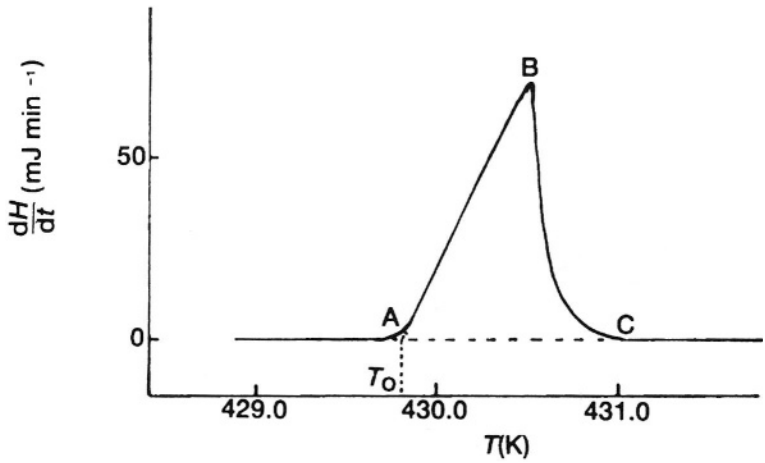

Figure 11.2
Idealized DSC record of melting of an impure sample. The slope of BF (=slope of AB in Figure 11.1) is used to correct the programmed temperature, T_p, to the sample temperature, T_s. T_m is the melting point. The area ABC is proportional to the enthalpy of fusion, ΔH_{fus}, of the sample. The fraction melted, F_n, at temperature T_n = area ADE/area ABC = a_n/A [2]. (With the permission of the Journal of Chemical Education.)

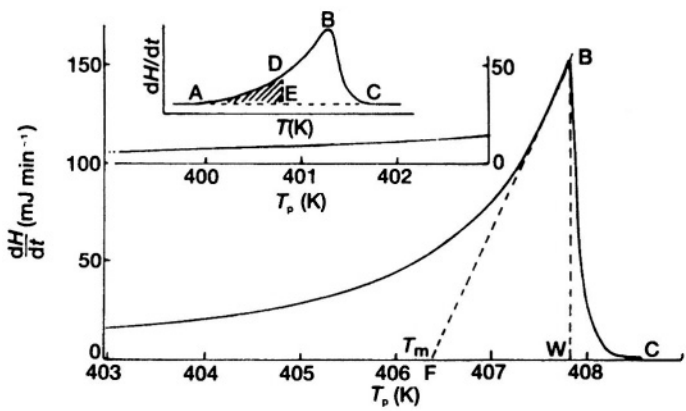

11.2 Phase equilibria

The simplest system to consider is that in which the impurity forms an ideal solution in the melt, i.e. a eutectic system. If the impurity is labelled, in the customary way, as component 2 and the solvent as component 1, then for equilibrium (at constant pressure) between pure 1 in the solid and 1 in the solution (or "melt") at activity a_1, there must be equality of the chemical potentials (μ) of 1 in the two phases:

$$\mu_1^\circ(\mathrm{s}) = \mu_1(\ell)$$

$$\mu_1^\circ(\mathrm{s}) = \mu_1^\circ(\ell) + RT \ln a_1 \qquad (11.1)$$

(where the superscript ° refers to standard conditions, i.e. unit activities). Differentiating equation (11.1) with respect to temperature, T:

$$\mathrm{d}\mu_1^\circ(\mathrm{s})/\mathrm{d}T = (\mathrm{d}\,\mu_1^\circ(\ell)/\mathrm{d}T) + R \ln a_1 + RT\,(\mathrm{d}(\ln a_1)/\mathrm{d}T)$$

and because $\mathrm{d}\mu/\mathrm{d}T = -\bar{S}$ (where the bar represents a molar quantity)

$$-\bar{S}_1^\circ(\mathrm{s}) = -\bar{S}_1^\circ(\ell) + R \ln a_1 + RT\,(\mathrm{d}(\ln a_1)/\mathrm{d}T) \qquad (11.2)$$

From equation (11.1)

$$R \ln a_1 = (\mu_1^\circ(\mathrm{s}) - \mu_1^\circ(\ell))/T$$

so equation (11.2) on rearranging, becomes:

$$\mathrm{d}(\ln a_1)/\mathrm{d}T = [-(\mu_1^\circ(\mathrm{s}) - \mu_1^\circ(\ell))/RT^2] - [(\bar{S}_1^\circ(\mathrm{s}) - \bar{S}_1^\circ(\ell))/RT]$$

$$= \{[(\mu_1^\circ(\ell) + T\bar{S}_1^\circ(\ell)] - [\mu_1^\circ(\mathrm{s}) + T\bar{S}_1^\circ(\mathrm{s})]\}/RT^2$$

or

$$\mathrm{d}(\ln a_1)/\mathrm{d}T = (\bar{H}_1^\circ(\ell) - \bar{H}_1^\circ(\mathrm{s}))/RT^2 = \Delta\bar{H}_{\mathrm{f},1}^\circ/RT^2 \qquad (11.3)$$

because $H = G + TS$ and $\bar{G}^\circ = \mu^\circ$. Integrating equation (13.3) between the limits $a_1 = 1$ at $T = T_o$ (because solid solutions are not formed) and $a_1 = a_1$ at $T = T$, assuming that $\Delta H_{\mathrm{f},1}^\circ$ is independent of temperature over the range:

$$\ln a_1 = (\Delta\bar{H}_{\mathrm{f},1}^\circ/R)[(1/T_o) - (1/T)]$$

For an ideal solution $a_1 = x_1$ (the mole fraction of 1). Hence

$$\ln a_1 = \ln (1 - x_2) = (\Delta \bar{H}_{f,1}^{\circ} / R)[(1/T_o) - (1/T)]$$

For a dilute solution, i.e. small values of x_2,

$$\ln (1 - x_2) \approx - x_2$$

$$x_2 = (\Delta \bar{H}_{f,1}^{\circ} / R)[(1/T) - (1/T_o)] \qquad (11.4)$$

Equation (11.4) forms the basis of melting-point depression calculations, as follows. At $T = T_m$, the melting point of the impure sample:

$$x_2 \approx (\Delta \bar{H}_{f,1}^{\circ} / R)[(T_o - T_m)/(T_o T_m)] = (\Delta \bar{H}_{f,1}^{\circ} / R)[\Delta T_f / (T_o T_m)] \qquad (11.5)$$

If ΔT_f is small, $T_o \approx T_m$ and $T_o T_m \approx T_o^2$. Also $x_2 = n_2/(n_1 + n_2) \approx m M_1/1000$, where m is the molality of the solute and M_1 the molar mass of the solvent. Hence:

$$\Delta T_f = [(R T_o^2 M_1)/(\Delta \bar{H}_{f,1}^{\circ} 1000)]\, m = K_f m$$

where K_f is termed the cryoscopic constant.

Only when the sample is completely melted, i.e. at $T >> T_m$, is the mole fraction of impurity in the liquid, x_2, the same as that in the original sample, x_2^*. From the phase diagram for a simple eutectic system (Figure 11.3) it may be seen that the value x_2^* is the minimum value which x_2 attains. At $T < T_m$ (see Figure 11.3), when the fraction of sample that has melted, F, is less than unity, the composition of the melt is closer to that of the eutectic, i.e., $x_2 > x_2^*$. When melting commences, the first liquid has the eutectic composition.

If F is the fraction melted at temperature T, then, assuming a linear initial segment of the liquidus curve (Figure 11.3), and using equation (11.4):

$$F = n_l/(n_l + n_s) = x_2^*/x_2 = (T_o - T_m)/(T_o - T) = (x_2^* R T_o^2)/[\Delta \bar{H}_{f,1}^{\circ} (T_o - T)] \qquad (11.6)$$

Rearrangement yields:

$$T = T_o - [x_2^* R T_o^2 / \Delta \bar{H}_{f,1}^{\circ}](1/F) \qquad (11.7)$$

If F can be determined at various temperatures, T, a plot of T against $1/F$ should yield a straight line, provided that $\Delta \bar{H}_{f,1}^{\circ}$ is independent of temperature. If the values of T_o and $\Delta \bar{H}_{f,1}^{\circ}$ are known, x_2^* can be determined from the measured slope of the line. The DSC curve is capable of providing values of F at temperatures T for use in such a plot.

Figure 11.3
Low concentration region of a simple eutectic phase diagram (inset) [2]. By the lever rule: $BC/AB = n_{solid}/n_{liquid}$. C is the composition of the melt in equilibrium with pure solid at T. Here $x_2 > x_2^*$. $F = n_\ell/(n_\ell + n_s) = AB/(AB + BC) = AB/BC = x_2^*/x_2$. (With the permission of the Journal of Chemical Education.)

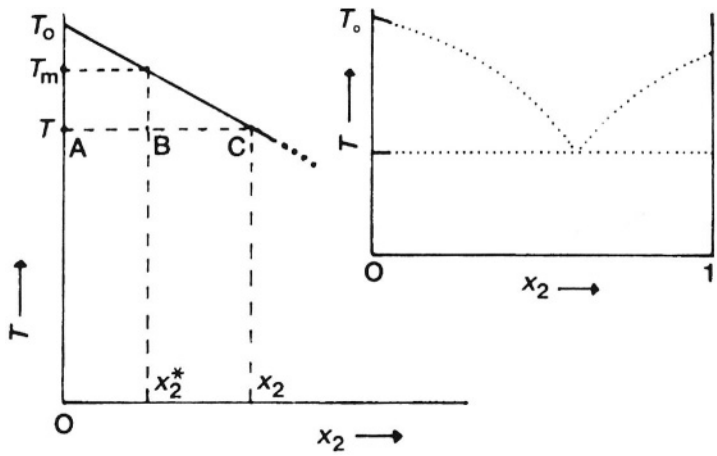

11.3 The DSC melting curve

The DSC measures the thermal energy per unit time, dH/dt, transferred to or from the sample as the temperature of the sample holder, T, is changed at a constant rate, $dT/dt = \beta$. Thus the output from the DSC is directly proportional to the heat capacity of the system, dH/dT.

$$dH/dt = (dH/dT)(dT/dt) \tag{11.8}$$

For an absolutely pure compound with zero melting range, dH/dt would become infinite at the melting point, T_o. For an impure compound, dH/dT is finite and is a function of T.

When the fraction melted, F, is zero, the heat capacity of the sample is that of the solid mixture, and when $F = 1$ the heat capacity of the sample is that of the ideal solution. Intermediate behaviour is obtained as follows:

$$dH/dT = (dH/dF)(dF/dT)$$

dF/dT is obtained from equation (11.6) as:

$$dF/dT = (x_2^* RT_o^2)/[\Delta\bar{H}_{f,1}^\circ (T_o - T)^2]$$

It is also assumed that, because of the restriction to consideration of ideal eutectic systems and to the formation of ideal solutions on melting, that:

$$H_F = F\,\Delta\bar{H}_{f,1}^{\circ}$$

and therefore:

$$dH/dF = \Delta\bar{H}_{f,1}^{\circ}$$

Combining these results:

$$dH/dT = (x_2^* RT_o^2)/(T_o - T)^2 \qquad (11.9)$$

Equation (11.9) then gives the variation of the heat capacity of the sample during melting as a function of T. The upper limit of the melting process is $T = T_m$ (when $F = 1$). Therefore, equation (11.7) becomes:

$$T_m = T_o - [x_2^* RT_o^2/\Delta\bar{H}_{f,1}^{\circ}]$$

The lower limit of the melting process is $T << T_o$, when $dH/dT \approx x_2^* R = C_s$, i.e. the heat capacity of the sample is approximately constant. In the idealized DSC curves given in Figs. 11.1 and 11.2, it has been assumed that the heat capacity of the liquid just above the melting temperature is the same as that of the solid at lower temperatures (i.e., both equal to C_s).

Equation (11.9) can be written as:

$$dH/dT = [x_2^* R(T_o/T)^2]/(T_o/T - 1)^2$$

so that, within the limits of the assumptions made above, the heat capacity during melting depends only on the mole fraction of impurity, x_2^* and the temperature relative to the melting point of the pure substance, T_o/T.

Because dH/dt is proportional to dH/dT, plots of dH/dT against T represent the initial part of an idealized DSC melting curve. Such curves for phenacetin and for benzamide, with values of x_2^* from 0.0050 to 0.3000, have been given by Marti *et al.* [5,6].

The real DSC melting curve, because of factors such as thermal lag, which is discussed in more detail below will look more like the curve in Figure 11.2, inset. The total area under the curve, i.e. area ABC, is proportional to the enthalpy of fusion, $\Delta H_{f,1}^{\circ}$. The actual value of $\Delta\bar{H}_{f,1}^{\circ}$ can be obtained by calibration of the instrument with a standard of known $\Delta H_{f,1}^{\circ}$ (Figure 11.1). The feature sought for the present discussion, the fraction of the sample melted, F, at temperature T, is obtained directly from the fractional area under the curve, i.e. F = area ADE/area ABC. The range of F values used in practice is usually restricted to $0.1 < F < 0.4$. Even with this restricted range, the linearity of plots of T against $1/F$ (equation (11.7)) is often poor. Corrections have to be made for thermal lag and for undetected premelting as discussed below.

11.4 Corrections

11.4.1 Thermal Lag

Flow of thermal energy from the holder at the programmed temperature, T_p, to the sample at a slightly lower temperature, T_s, is governed by Newton's law:

$$T_p - T_s = (dH/dt)\, R_o \qquad (11.10)$$

where R_o is the thermal resistance. The value of R_o for the instrument may be obtained [7] from the melting curve of a high purity standard (Figure 11.1). This will melt over a very narrow temperature range, so that as the programmed temperature continues to increase with time, the sample temperature, T_s, will remain constant, i.e. $dT_s/dt = 0$. From equation (11.10):

$$(dT_p/dt) - (dT_s/dt) = R_o\, [d(dH/dt)/dt]$$

Hence:

$$(dT_p/dt) = R_o\, [d(dH/dt)/dt] = R_o\, (dT/dt)\, [d(dH/dt)/dT] = R_o\, \beta\, [d(dH/dt)/dT]$$

and

$$d(dH/dt)/dT = R_o$$

R_o may thus be determined from the slope, AB, of the DSC melting curve for the high purity standard (Figure 11.1). The value of R_o is then used graphically or analytically to correct the programmed temperature, T_p, to the true sample temperature, T_s. T_s then, rather than T_p, is plotted against $1/F$.

11.4.2 Undetermined Premelting

Even with correction for thermal lag, the linearity of the plots of T_s against $1/F$ is often not good, and corrections have to be made to the measured areas, for melting which has occurred at lower temperatures and which is difficult or impossible to measure. This is evident in the small but cumulatively significant deviation from the ideal baseline illustrated in Figure 11.2.

If the undetermined area under the curve is ϵ, the measured partial areas up to temperatures $T_1, T_2 \ldots\ldots T_n$ are $a_1, a_2 \ldots\ldots a_n$, respectively, and the measured total area is A, the true value of F_n is:

$$F_n = (a_n + \epsilon)/(A + \epsilon)$$

or

$$1/F_n = (A + \epsilon)/(a_n + \epsilon) \approx (A)/(a_n + \epsilon)$$

because $A >> \epsilon$, so the effect of including ϵ is to reduce the value of $1/F_n$, see Figure 11.4. In practice ϵ is treated as a parameter whose value is adjusted so that a plot of T_s against the corrected $1/F$ is linear, see Figure 11.4. The restraints are that the final value of $(A + \epsilon)$ should correspond directly to the correct value of $\Delta H_{f,1}^{\circ}$ (if known) and that the value of T_o, determined from the intercept on the T_s axis, should be correct. Once these conditions have been met, the value of x_2^* (= slope x $\Delta H_{f,1}^{\circ}/RT_o^2$) and hence the purity of the sample can be determined. Because melting actually begins at the eutectic temperature, which may be far below the range of temperatures being examined, the correction, ϵ, may sometimes be quite large and values of as much as 30% of the total area are not uncommon [8]. Obviously the approximation, $A + \epsilon \approx A$, cannot then be used. Sondack [9] has suggested an alternative procedure.

Figure 11.4
Correction for undetermined premelting. The correction = 100 x ϵ/A and $F = (a + \epsilon)/(A + \epsilon)$ [2]. (With the permission of the Journal of Chemical Education.)

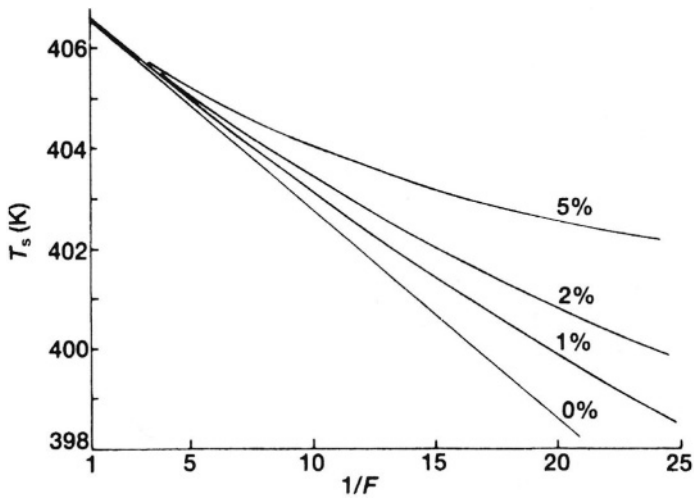

The whole procedure for purity determination is summarized in the flowchart (Figure 11.5). More details on the procedure are given in references [3,9].

Figure 11.5
Flow chart representing the procedure used in purity determination by DSC [2].
(With the permission of the Journal of Chemical Education.)

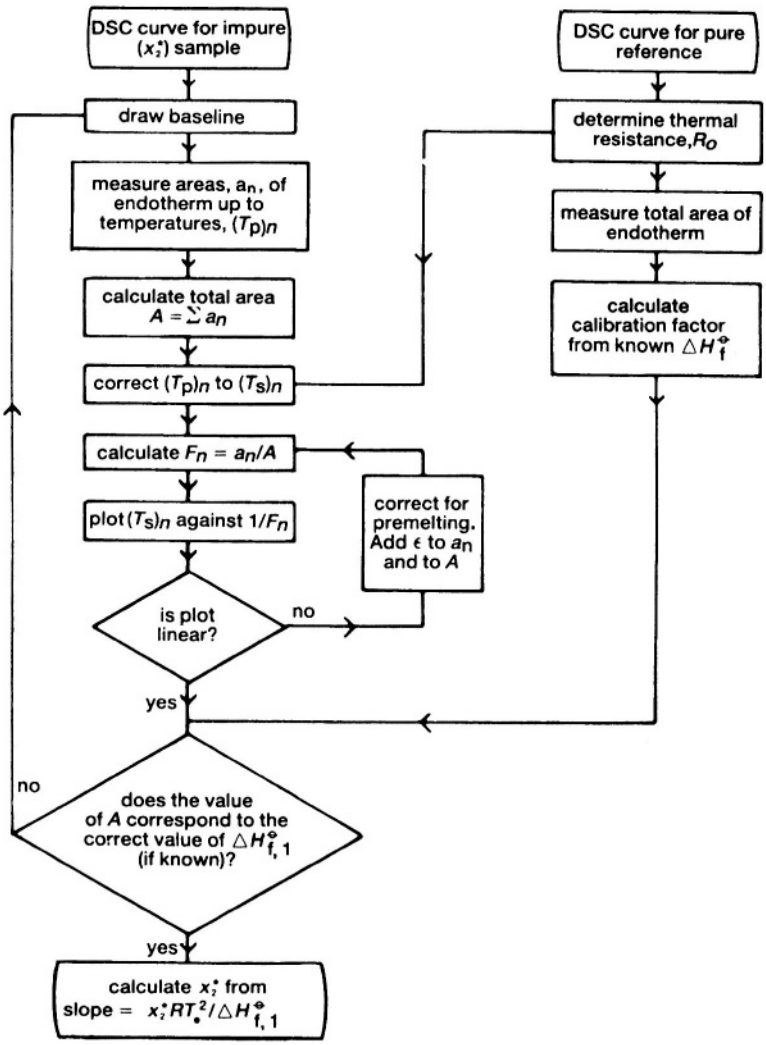

11.5 Step methods

Staub and Perron [10] have shown that a stepped heating technique can extend the working region for purity determination. The sample is heated through the melting region in steps of a few tenths of a degree, thus allowing a closer approach to true thermodynamic equilibrium. The results of such a procedure [11] on an impure phenacetin sample, using a modified DSC-1B are shown in Figure 11.6. There are six steps/5 K and the areas of each peak, obtained by integration, are given. The first eleven peaks and the last three arise from the difference in the heat capacity of the sample and reference. These peaks have approximately constant area and the melting peaks can be corrected for this difference. Because thermal equilibrium is established after each peak, no correction is required for the thermal resistance, R_o, of the system. The corrected areas of all the melting steps are then summed and converted to fractional areas, F and $1/F$ is plotted against T, as before, except that with this procedure [11] all the data are used including the latter part of the melting process. The linearization process for the undetermined premelting still has to be carried out. Gray and Fyans [8] have suggested an alternative procedure to that given above, in which the mole fraction of impurity (x_2^*) is calculated from the areas of two consecutive stepped peaks (a_n and a_{n-1}), the magnitude of the stepping interval (ΔT), and the molar mass (M) and the melting point (T_o) of the pure major component. This method depends upon the applicability of the van't Hoff equation and the relationship derived [8] is:

$$x_2^* = [2M\,\Delta T/\,RT_o^2][(a_n\,a_{n-1})(a_n + a_{n-1})/(a_n - a_{n-1})^2]$$

The melting point (T_o) of the pure solvent may be determined [11] from the areas a_n and a_{n-1}, the step interval ΔT and the final temperature of the step T_n:

$$T_o = T_n + [\,2\,\Delta T\;a_{n-1}/(a_n - a_{n-1})]$$

It is recommended [8] that step increments used should be as large as possible. Elder [12] has compared results obtained using the isothermal step method with those using the dynamic method and discusses the advantages and disadvantages.

11.6 Conclusions

Moros [13] has discussed the design, preparation, and evaluation of phenacetin doped with different amounts of aminobenzoic acid as standards for checking the reliability of purity determinations by DSC. The precision, accuracy and the limits of applicability of the method have been discussed by Hunter and Blaine [14]. Raskin [15], in a critical review of methods of purity determination using DSC, concludes that the accuracy of the method is generally overestimated. A realistic estimate of the accuracy in the range $0.005 < x^{2*} < 0.02$ is given [15] as 30-50% when the sample mass is less than 3 mg and the scanning rate is less than 2 K min^{-1}.

Figure 11.6
Stepwise heating of an impure (96.04 mole %) phenacetin sample [11]. Peak areas are expressed in thousands. (With the permission of the American Chemical Society.)

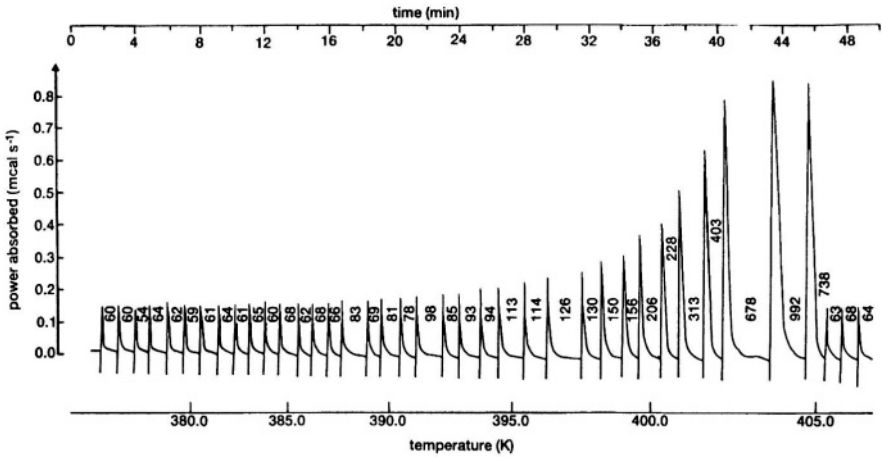

Garn *et al.* [16-18] have discussed the problems that arise when there is appreciable solid solubility. They used NMR to detect the solidus and compared DSC and NMR results. They showed that lack of thermal equilibrium is not a principal source of error in the method and also found that the measured impurity content is sometimes dependent upon the nature of the impurity as well as its concentration. McGhie [19] has provided a very useful discussion of the melting behaviour of solid solutions, using a system consisting of 0 to 20% anthracene in 2,3-dimethyl naphthalene as an example. The normal DSC method is invalid for such systems.

Wiedemann [20] has described the use of simultaneous DSC-thermomicroscopy (see Chapter 5)for purity detemination. The addition of thermomicroscopy allows the various stages of melting to be photographed to show the changes that occur. Flammersheim et al. [21] have discussed the correction of DSC curves for the broadening of peaks caused by the particular apparatus.

Purity determinations by thermal measurements are competitive [22] with other techniques in terms of accuracy, precision, and ease of measurement, and, in many cases, e.g. for crystalline organic compounds, are superior.

References

1. P.W. Atkins, "Physical Chemistry", Oxford University Press, Oxford, 6th Edn, 1998, p.179.
2. M.E. Brown, J. Chem. Educ., 56 (1979) 310.
3. R.L. Blaine and C.K. Schoff (Eds), "Purity Determinations by Thermal Methods", ASTM Special Technical Publication 838, American Society for Testing and Materials, Philadelphia, 1984.
4. W.P. Brennan, M.P. Divito, R.L. Fyans and A.P. Gray, in "Purity Determinations by Thermal Methods", (Eds R.L. Blaine and C.K. Schoff), ASTM Special Technical Publication 838, American Society for Testing and Materials, Philadelphia, 1984, p.5.
5. E.E. Marti, Thermochim Acta, 5 (1973), 173.
6. E.E. Marti, O. Heiber, W. Huber and G. Tonn, Proc. 3rd ICTA, (Ed. H.G. Weidemann), Birkhauser Verlag, Basel, 1971, Vol.3, p.83.
7. Thermal Analysis Newsletters, Nos.5 and 6, Perkin-Elmer Corporation, Norwalk, Connecticut (undated).
8. A.P. Gray and R.L. Fyans, Thermal Analysis Application Study No. 10, Perkin-Elmer, Norwalk, 1973.
9. D.L. Sondack, Anal. Chem., 44 (1972) 888.
10. H. Staub and W. Perron, Anal. Chem., 46 (1974) 128.
11. J. Zynger, Anal. Chem., 47 (1975) 1380.
12. S.A. Moros, in "Purity Determinations by Thermal Methods", (Eds R.L. Blaine and C.K. Schoff), ASTM Special Technical Publication 838, American Society for Testing and Materials, Philadelphia, 1984, p.22.
13. J.E. Hunter III and R.L. Blaine, in "Purity Determinations by Thermal Methods", (Eds R.L. Blaine and C.K. Schoff), ASTM Special Technical Publication 838, American Society for Testing and Materials, Philadelphia, 1984, p.39.
14. J.P. Elder, in "Purity Determinations by Thermal Methods", (Eds R.L. Blaine and C.K. Schoff), ASTM Special Technical Publication 838, American Society for Testing and Materials, Philadelphia, 1984, p.50.
15. A.A. Raskin, J. Thermal Anal., 30 (1985) 901.
16. P.D. Garn, B. Kawalec, J.J. Houser and T.F. Habash, Proc. 7th ICTA, Vol.2, Wiley, Chichester, 1982, p.899.
17. B. Kawalec, J.J. Houser and P.D. Garn, J. Thermal Anal., 25 (1982) 259.
18. T.F. Habash, J.J. Houser and P.D. Garn, J. Thermal Anal., 25 (1982) 271.
19. A.R. McGhie, in "Purity Determinations by Thermal Methods", (Eds R.L. Blaine and C.K. Schoff), ASTM Special Technical Publication 838, American Society for Testing and Materials, Philadelphia, 1984, p.61.
20. H.G. Wiedemann, R. Riesen and G. Bayer, in "Purity Determinations by Thermal Methods", (Eds R.L. Blaine and C.K. Schoff), ASTM Special Technical Publication 838, American Society for Testing and Materials, Philadelphia, 1984, p.107.

21. H.J. Flammersheim, N. Eckhardt and W. Kunze, Thermochim. Acta, 187 (1991) 269.
22. C.K. Schoff, in “Purity Determinations by Thermal Methods”, (Eds R.L. Blaine and C.K. Schoff), ASTM Special Technical Publication 838, American Society for Testing and Materials, Philadelphia, 1984, p. 141.